

Natural Wake-Sleep Algorithm

Csongor Varady^{1,2}, Riccardo Volpi¹, Luigi Malagò¹, and Nihat Ay²

¹ Romanian Institute for Science and Technology University, Cluj-Napoca, Romania

² Max Planck Institute for Mathematics in the Sciences, Leipzig, Germany

Abstract. The benefits of using the natural gradient are well known in a wide range of optimization problems. However, for the training of common neural networks the resulting increase in computational complexity sets a limitation to its practical application. Helmholtz Machines are a particular type of generative model composed of two Sigmoid Belief Networks (SBNs), acting as an encoder and a decoder, commonly trained using the Wake-Sleep (WS) algorithm and its reweighted version RWS. For SBNs, it has been shown how the locality of the connections in the graphical structure induces sparsity in the Fisher information matrix. The resulting block diagonal structure can be efficiently exploited to reduce the computational complexity of the Fisher matrix inversion and thus compute the natural gradient exactly, without the need of approximations. We present a geometric adaptation of well-known methods from the literature, introducing the Natural Wake-Sleep (NWS) and the Natural Reweighted Wake-Sleep (NRWS) algorithms. We present an experimental analysis of the novel geometrical algorithms based on the convergence speed and the value of the log-likelihood, both with respect to the number of iterations and the time complexity and demonstrating improvements on these aspects over their respective non-geometric baselines.

Keywords: Natural Gradient · Helmholtz Machines · Wake-Sleep Algorithm · Sigmoid Belief Networks · Generative Models.

1 Introduction

Deep generative models have been successfully employed in unsupervised learning to model complex and high dimensional distributions thanks to their ability to extract higher-order representations of the data and thus they generalize better [20, 8]. An approach which proved to be successful and thus common to several models is based on the use of two separate networks: the recognition network, i.e., the encoder, which provides a compressed latent representation for the input data, and the generative network, i.e., the decoder, able to reconstruct the observation in output. AutoEncoders (AEs) [15] are a classical example of this paradigm, where both the encoder and the decoder are deterministic feed-forward networks. Variational AutoEncoders (VAEs) [22, 31] introduce an approximate posterior distribution over the latent variables which are then sampled, thus being modelled as stochastic networks. Helmholtz Machines

(HM) [11] consist of a recognition and a generative network both modelled as a Sigmoid Belief Network (SBN) [28], and differently from standard VAEs, are characterized by discrete hidden variables.

The training of stochastic networks is a challenging task in deep learning [14]. This applies in particular to generative models based on stochastic networks, usually trained by the maximization of the likelihood or similarly by the minimization of a divergence function between the unknown distribution of the data and that of the generative model. The challenges for optimization are due to the presence of terms which are computationally expensive to be estimated, such as the partition function. A solution to this problem consists in the introduction of a family of tractable approximate posterior distributions which, in the presence of continuous hidden variables for which the stochastic back-propagation of the gradient is possible. This allows training the two networks of a VAE simultaneously, through the definition of a unique loss function which corresponds to a lower-bound for the likelihood, i.e., the ELBO. In the presence of discrete hidden variables, as for HMs, this approach cannot be directly employed, and thus standard training procedure relies on the well-known Wake-Sleep [19] algorithm, in which two optimization steps for the parameters of the recognition and generative networks are alternated. The Wake-Sleep algorithm, as well as more recent advances [10, 9, 33, 18], relies on the conditional independence assumption between the hidden variables of each layer, associated with the directed graphical model nature of a SBN. This leads to a computationally efficient formula for the weights update which does not require the gradients to be back-propagated through the full network.

Besides the choice of the specific loss function to be optimized, depending on the nature of the generative model, in the literature several approaches to speed up the convergence during training have been proposed, through the definition of different training algorithms. One line of research, initiated by Amari and co-workers [3, 2], takes advantage of a geometric framework based on notions of Information Geometry [5], which allows the definition of the natural gradient, i.e., the Riemannian gradient of the loss function for a neural network computed with respect to the Fisher-Rao metric. In this paper, we pursue this line of research. In general the computation of the natural gradient requires the inversion of an estimation of the Fisher information matrix, and for this reason it cannot be directly applied for the training of large neural network due to its computation costs. Several alternatives have been proposed in the literature [12, 13, 17, 29, 27, 32] which are all based on more or less sophisticated approximations of the structure of the Fisher information matrix, by introducing (conditional) independence assumptions between random variables which allows its efficient inversion. The use of the natural gradient for the training of generative models has been exploited in particular in [26, 34].

In this paper we follow a different approach for the computation of the natural gradient for the training of a HM which does not require the use of an approximate Fisher information matrix before its empirical evaluation. Indeed, motivated by preliminary results from [6] for the computation of the Fisher

information matrix for a SBN, we observe that the Fisher information matrix associated with the joint statistical model represented by a HM takes a block diagonal structure, where the block sizes depend linearly on the size of each hidden layer. This result, which can be seen as a consequence of the topology of the directed graphical model associated to the SBN, does not require the introduction of any additional independence assumption between random variables in the Fisher matrix. Notice that the level of sparsity for the Fisher matrix in SBNs is superior to the standard assumption of independence between layers, where the size of the blocks are quadratic in the size of each hidden layer, thus allowing a more computationally efficient inversion of the Fisher matrix. Motivated by these observations we propose a geometric version of both the Wake-Sleep and the Reweighted Wake-Sleep algorithms for the training of HMs, where the gradient is replaced by the corresponding natural gradient. The intrinsic sparsity of the Fisher matrix, which is a direct consequence of the topology of the network, limits the impact on the cost per iteration. This has the advantage to allow for an exact computation of the natural gradient not requiring further assumptions, thus taking advantage of the speed-up in convergence during training, still limiting the computational overhead.

The paper is organized as follows. First in Section 2 we will briefly introduce the Wake-Sleep and the Reweighted Wake-Sleep algorithms. In Sections 3 and 4 we will introduce the natural gradient and the Fisher matrix, describing its block structure in the case of a HM. In Section 5 we will define the Natural Wake-Sleep Algorithm. Finally in Sections 6 and 7 we will discuss some results and draw our conclusions.

2 The Reweighted Wake-Sleep Algorithm

A Helmholtz Machine is composed by two Sigmoid Belief Networks, a generative network p depending on weights and biases θ and a recognition (or inference) network q , depending on weights and biases ϕ . Following a reinterpretation due to [10], the training of Helmholtz Machines can be recast in terms of a variational objective [16, 22]. This is analogous to the learning in a Variational Autoencoder [22] which requires maximizing a lower bound of the likelihood. The derivative of the log-likelihood of x can be approximated with a Monte Carlo sampling [10, 24]

$$\begin{aligned} \frac{\partial \ln p(x)}{\partial \theta} &= \frac{1}{p(x)} \mathbb{E}_{h \sim q(h|x)} \left[\frac{p(x, h)}{q(h|x)} \frac{\partial \ln p(x, h)}{\partial \theta} \right] \\ &\simeq \sum_{k=1}^K \tilde{\omega}_k \frac{\partial \ln p(x, h^{(k)})}{\partial \theta} \quad \text{with } h^{(k)} \sim q(h|x). \end{aligned} \tag{1}$$

This is called **p-wake update**. $q(h|x)$ is the approximate posterior (given by the recognition network), while the last step is involving the Monte Carlo ap-

proximation of the expectation value with importance weights

$$\tilde{\omega}_k = \frac{\omega_k}{\sum_{k'} \omega_{k'}}, \text{ with } \omega_k = \frac{p(x, h^{(k)})}{q(h^{(k)}|x)} \quad (2)$$

Equation (1) is also referred to as Reconstruction Likelihood (RL) and the optimization is performed in function of the parameters of the generation network θ . The approximate posterior depends also from another set of parameters ϕ . q can be optimized by minimizing the variance of the Monte Carlo estimation in Eq. (1), i.e., minimizing the KL divergence with the generative posterior [10, 24]. This can be averaged sampling x from the true data distribution $p_{\mathcal{D}}(x)$ (**q-wake update**)

$$- \frac{\partial K L[p(\cdot|x)||q(\cdot|x)]}{\partial \phi} \simeq \sum_{k=1}^K \tilde{\omega}_k \frac{\partial \ln q(h^{(k)}|x)}{\partial \phi} \quad \text{with } h^{(k)} \sim q(h|x) \quad (3)$$

or it can be averaged over samples x, h from the generative model $p(x, h)$ (**q-sleep update**)

$$- \mathbb{E}_p \left[\frac{\partial K L[p(\cdot|x)||q(\cdot|x)]}{\partial \phi} \right] \simeq \sum_{k=1}^K \frac{\partial \ln q(h^{(k)}|x^{(k)})}{\partial \phi} \quad \text{with } x^{(k)}, h^{(k)} \sim p(x, h). \quad (4)$$

The algorithm just described is called Reweighted Wake-Sleep (RWS) [10, 24]. The q-sleep update it is commonly known as sleep phase in the classical Wake-Sleep (WS) [11, 19] algorithm, which only uses the p-wake update and the q-sleep update, both with 1 sample.

3 Natural Gradient

Information Geometry [1, 5, 4, 7] studies the geometry of statistical models using the language of Riemannian geometry, representing a set of probability distributions $\mathcal{M} = \{p = p_{\theta} : \theta \in \Theta\}$ as a manifold. The parameterization θ for p identifies a set of coordinates, i.e., a chart, over the manifold. Similarly, it is possible to define the tangent space $T_p \mathcal{M}$ in each point as the set of the velocity vectors along all the curves which pass through in p . In Information Geometry, statistical manifolds are commonly endowed with a Riemannian Fisher-Rao metric over the tangent bundle defined by the expected value in p of the product of two tangent vectors, represented by centered random variables. Given a basis for the tangent space, derived from the choice of the parameterization, the inner product associated to the Fisher-Rao metric is represented though a quadratic form expressed through the Fisher information matrix F . Given a real-valued function \mathcal{L} defined over the statistical manifold \mathcal{M} , the direction of steepest ascent is represented by the Riemannian gradient of \mathcal{L} whose evaluation depends on the metric. Let $\nabla \mathcal{L}$ denote the vector of partial derivatives $\frac{\partial}{\partial \theta} \mathcal{L}(p)$. These represent the coordinates of a covector, $\frac{\partial}{\partial \theta} \mathcal{L}(p) \in T_p^* \mathcal{M}$. The natural gradient is

the vector in $T_p\mathcal{M}$ associated to $\nabla\mathcal{L}$ through the canonical isomorphism between tangent and cotangent space induced by the metric [3, 2], i.e.

$$\tilde{\nabla}\mathcal{L}(\theta) = F(\theta)^{-1}\nabla\mathcal{L}(\theta), \quad (5)$$

with

$$F(\theta) = \mathbb{E}_p \left[\frac{\partial}{\partial\theta} \log p(\theta) \left(\frac{\partial}{\partial\theta} \log p(\theta) \right)^{\top} \right] = -\mathbb{E}_p \left[\frac{\partial^2}{\partial\theta\partial\theta} \log p(\theta) \right]. \quad (6)$$

The natural gradient descent update then takes the form of

$$\theta_{t+1} = \theta_t - \eta \tilde{\nabla}\mathcal{L}(\theta), \quad (7)$$

where θ_t are the weights at step t and η is the learning rate.

4 Fisher Information Matrix for Helmholtz Machines

The computation of the Fisher information matrix, needed in order to compute the natural gradient of a given loss function, strongly depends on the nature of the statistical model with respect to which the loss is defined. We refer the reader to [30] for the computation in the case of feed-forward networks for classification and regression problems. In this section we show how the Fisher information matrix in Eq. (6) can be rewritten in the case of Sigmoid Belief Networks (SBN), which constitute the building blocks for Helmholtz Machines.

The Fisher information matrix for directed acyclic graphical models takes a simplified block diagonal form thanks to the locality of connection matrix, given by the conditional independence the random variables. This result has been exploited recently in the training of stochastic feed-forward neural networks, see for instance Thm. 3 from [32], leading to a block-diagonal Fisher matrix, with one block per layer. However, by a direct generalization to deep stochastic networks of a result from [6] for two-layers networks, it is easy to show that SBNs admit a Fisher information matrix with a finer-grained block structure. The following proposition formalizes this result, while Fig. 1 provides a graphical representation.

Proposition 1. *Let \mathcal{G} be a directed acyclic graphical model, whose variables are grouped in layers such that each node from the i -th layer has parent nodes from the $(i - 1)$ -th layer only. The Fisher information matrix associated to the joint probability distribution p that factorizes as the product of conditional distribution according to \mathcal{G} has a block-diagonal structure, with blocks for each hidden unit of size equal to the number of parent nodes.*

The proof of this result is based on a generalization of Lemma 1 from [6], see also Appendix A for more details.

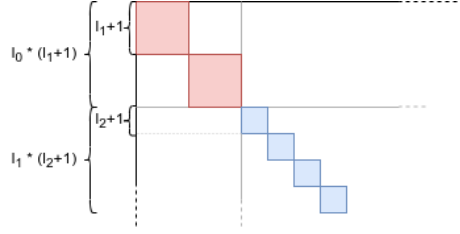


Fig. 1: Graphical representation of the Fisher information matrix for Sigmoid Belief Networks. The gray lines correspond to the blocks associated to the layers of the network. The matrix admits a fine-grained block-diagonal structure with blocks of size equal to the size of the hidden layers.

Let us consider a Helmholtz Machine with L layers $h^{(i)}$, $h^{(0)} = x$ is also called the visible layer. The generative network introduces a prior on the top most layer L leading to the factorization

$$p_{\theta}(x, h) = p_{W^{(L)}}(h^{(L)}) \prod_{i=L-1}^0 p_{W^{(i)}}(h^{(i)} | h^{(i+1)}), \quad (8)$$

and it is parameterized by weights and biases $W^{(i)}$ at each layer i . The recognition network targets to approximate the true posterior distribution by

$$q_{\phi}(h|x) = \prod_{i=1}^L q_{V^{(i)}}(h^{(i)} | h^{(i-1)}). \quad (9)$$

parameterized by weights and biases $V^{(i)}$ at each layer i . By means of the generative and discriminative networks we can define two different joint distributions over the visible and hidden variables $p_{\theta}(x, h)$ and $q_{\phi}(x, h) = q_{\phi}(h|x)p(x)$ which correspond to the statistical manifolds for which we are interested in computing the Fisher matrices.

Let i denote the layer, and j one of its hidden nodes, we denote with $W_j^{(i)}$ the j -th columns of the matrix $W^{(i)}$. Then the blocks associated to the i th-layer and j -th hidden unit read

$$F_{p,j}^{(i)} = \mathbb{E}_{p(x,h)} \left[\sigma(W_j^{(i)} h^{(i+1)}) \left(1 - \sigma(W_j^{(i)} h^{(i+1)}) \right) h^{(i+1)} h^{(i+1)\text{T}} \right], \quad (10)$$

$$F_{q,j}^{(i)} = \mathbb{E}_{q(x,h)} \left[\sigma(V_j^{(i)} h^{(i-1)}) \left(1 - \sigma(V_j^{(i)} h^{(i-1)}) \right) h^{(i-1)} h^{(i-1)\text{T}} \right]. \quad (11)$$

Each block of the Fisher matrix can then be estimated by Monte Carlo sampling based on n samples coming from the observations for $F_{q,j}^{(i)}$, or sampled from the prior for $F_{p,j}^{(i)}$. In the following notice that $h^{(i)}$ is a stochastic quantity depending through the forward pass on the input to the network, thus Eqs. (10) and (11)

can be estimated by Monte Carlo methods, that is

$$F_{p,j}^{(i)} \approx \frac{1}{n} \sum \sigma(W_j^{(i)} h^{(i+1)}) \left(1 - \sigma(W_j^{(i)} h^{(i+1)})\right) h^{(i+1)} h^{(i+1)\text{T}} \quad (12)$$

$$= \left(H^{(i+1)}\right)^T Q_p^{(i+1)} H^{(i+1)}, \quad (13)$$

$$F_{q,j}^{(i)} \approx \frac{1}{n} \sum \sigma(V_j^{(i)} h^{(i-1)}) \left(1 - \sigma(V_j^{(i)} h^{(i-1)})\right) h^{(i-1)} h^{(i-1)\text{T}} \quad (14)$$

$$= \left(H^{(i-1)}\right)^T Q_q^{(i-1)} H^{(i-1)}, \quad (15)$$

where σ is the sigmoid function, used in SBN. In the last step we introduced a matrix representation for the estimation of the Fisher matrix, where the $H^{(i)}$ matrices are obtained by concatenating for each sample the $h^{(i)}$ vector as a row vector, while the diagonal matrices $Q_p^{(i)}$ and $Q_q^{(i)}$ depends on the evaluation of the activation function. Eqs. (13) and (15) represent the blocks of the full Fisher matrix, for $W_j^{(i)}$ and for $V_j^{(i)}$, respectively. This block structure is very convenient and represents the main argument for its practical application. Notice that the empirical estimations in Eqs. (13) and (15) are not to be confused with the approximations typically introduced for the simplification of the Fisher matrix, needed to make it computational tractable in feed-forward neural networks. In the following sections we will discuss in more detail the feasibility of the computation of the blocks of the Fisher matrix and their inversion, together with an analysis of the computational complexity of the proposed algorithm.

The Fisher matrices in Eqs. (10) and (11) only depend on the statistical models associated to the joint distributions $p(x, h)$ and $q(x, h)$, and in particular they are independent from the specific loss function \mathcal{L} or its vector of partial derivatives $\nabla \mathcal{L}$, as well as from the chosen training algorithm. Hence, since the model of the Helmholtz Machine remains unchanged, the same Fisher metrics can be used for both the WS and RWS algorithms.

It is worth mentioning that the Fisher information matrix of the visible distribution $p(x|h)$ could also be derived and used for training, which could be better for approximating the real distribution of the data $p(x)$. This derivation however presents additional complications and its computational feasibility will be explored in future works.

5 The Natural Reweighted Wake-Sleep Algorithm

In this section we introduce the Natural Reweighted Wake-Sleep (NRWS) algorithm, a geometric adaptation of the Reweighted Wake-Sleep (RWS) algorithm, where the update of the weights is obtained thorough the computation of the natural gradient of the different loss functions in the wake and sleep updates. The algorithm is characterized by a hyperparameter s associated to the number of samples drawn from the approximate posterior $q(h|x)$ for each x . Similarly to the Reweighted Wake-Sleep, for which the standard Wake-Sleep algorithm is

obtained in case $s = 1$ and only the sleep phase q-update is used, under the same conditions NRWS reduces to the Natural Wake-Sleep algorithm (NWS).

The pseudo-code of NRWS is presented in Alg. 1. Besides the number of samples s and learning rate η , two other hyperparameters have been introduced: a damping factor α needed to invert the estimation of the Fisher information matrix computed from the samples when it is not full rank, and the number of steps K during which the Fisher information matrix is frozen, i.e., it is not updated with respect to the new batch, for computational efficiency.

Algorithm 1: Natural Reweighted Wake-Sleep

- 1 Let x be a batch of samples from the dataset
 - 2 Let p and q be the joint distributions of the generation and the recognition networks with weights w and v respectively
 - 3 Let ω_K be the importance weights from the RWS algorithm
 - 4 Let L be the depth of the HM
 - 5 **Wake phase update**
 - 6 **for** each layer i from q ascending with $h_0 = x$ **do**
 - 7 Sample $h^{(i+1)}$ from $q(h^{(i+1)}|h^{(i)})$
 - 8 Compute the probability distribution $p(h^{(i)}|h^{(i+1)})$ of a sample $h^{(i)}$ from p
 - 9 Compute the gradients $g_p^{(i)}$ with respect to w_i
 - 10 Compute the $(F_p^{(i)})^{-1}$ for the sub-blocks in i with $h^{(i+1)}$ and $p(h^{(i)}|h^{(i+1)})$
 - 11 q -wake update:
 - 12 Calculate $g_q^{(i)}$ and $(F_q^{(i)})^{-1}$ similarly to the *Sleep* phase
 - 13 Compute $\hat{g}_p^{(i)}, \hat{g}_q^{(i)}$ by applying the weights ω_K to $g_p^{(i)}$ and $g_q^{(i)}$
 - 14 $\tilde{g}_p^{(i)} = (F_p^{(i)})^{-1} \hat{g}_p^{(i)}$
 - 15 $\tilde{g}_q^{(i)} = (F_q^{(i)})^{-1} \hat{g}_q^{(i)}$
 - 16 Apply the gradients \tilde{g}_i^p and \tilde{g}_i^q to w and v
 - 17 **Sleep phase update**
 - 18 **for** each layer i from p descending with h_L sampled from the prior **do**
 - 19 Sample $h^{(i-1)}$ from $p(h^{(i-1)}|h^{(i)})$
 - 20 Compute the probability distribution $q(h^{(i)}|h^{(i-1)})$ of a sample $h^{(i)}$ from q
 - 21 Compute the gradients $g_q^{(i)}$ with respect to v_i
 - 22 Compute the $(F_q^{(i)})^{-1}$ for the sub-blocks in i with $h^{(i-1)}$ and $q(h^{(i)}|h^{(i-1)})$
 - 23 $\tilde{g}_q^{(i)} = (F_q^{(i)})^{-1} g_q^{(i)}$
 - 24 Apply the gradients \tilde{g}_i^q to v
-

5.1 Inversion of the Fisher Matrix

The matrices $H^T Q H$ associated with the estimation of the Fisher blocks from Eqs. (13) and (15) may be singular depending on the number of samples n in the batch used in the estimation compared its size, which depends on the size

l_i of each layer i . During training n is the size of the mini-batch multiplied by the number of samples from the network (respectively p or q , depending on the Fisher matrix under consideration). Notice that during training typically $s < l_i$, thus to guarantee the invertibility we add a damping factor $\alpha > 0$ multiplying the identity matrix in addition to $H^T Q H$.

$$\tilde{F} = \frac{\alpha \mathbb{1}_l + F}{1 + \alpha} \quad (16)$$

so that $\tilde{F}^{-1} \rightarrow \mathbb{1}_l$ for $\alpha \rightarrow \infty$ and $\tilde{F}^{-1} \rightarrow F^{-1}$ for $\alpha \rightarrow 0$. Notice that there is no need to compute explicitly the Fisher matrix nor its inverse in the computation of the natural gradient, since depending on the s and l_i it may be more convenient to keep in memory its rank- k update representation.

Now that we can use the Sherman-Morrison formula to calculate the inverse of a rank- k update

$$\left(\frac{\alpha \mathbb{1}_l + H^T Q H}{1 + \alpha} \right)^{-1} = \frac{1 + \alpha}{\alpha} (\mathbb{1}_l - H^T (\alpha Q^{-1} + H H^T)^{-1} H) . \quad (17)$$

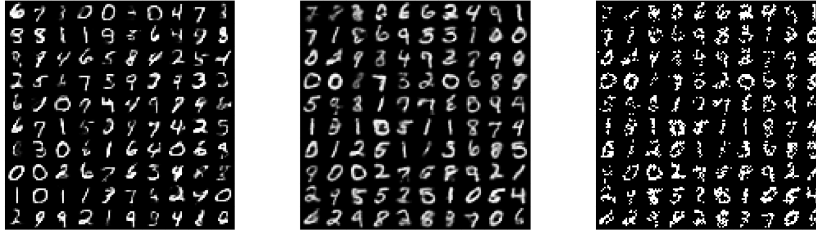
By using the Sherman-Morrison instead of a straightforward matrix inversion, we reduce the theoretical complexity of the algorithm from $\mathcal{O}(l^3)$ to $\mathcal{O}(ln^2)$ where l is the length of the largest layer in the network and n is the number of samples from the joint distribution. A direct consequence of this operation is that overall complexity will be bounded by $\mathcal{O}(l_0 l_1 n^2)$ where l_0 and l_1 are the bottom two layers of the Helmholtz Machine, which are usually the largest.

Even using all the expedients explained so far, calculating the inverse of the Fisher matrix is still adding computational complexity on the training algorithm. Assuming the locality of the gradient descent learning step, we make the approximation of slowly changing metric during few training steps. Under these assumptions we can reuse the Fisher matrix for a certain amount of steps K , without recalculating it. We will call this technique, K-step update.

6 Experiments

To quickly explore the ranges of the hyperparameters (more details in Appendix B), we use a downsized binarized version of the MNIST dataset, from $28 * 28$ to $14 * 14$ which we call the miniMNIST dataset (Fig. 2), similar to the one used by Hinton et. al. [19]. This is mainly used to explore the ranges of the hyperparameters quicker and serves as a quick comparison between the models WS, RWS and NRWS.

For the final performance evaluation of NRWS we use the binarized version of the MNIST database of handwritten digits [25], which is a standard comparison benchmark for many SBNs, including the Reweighted Wake-Sleep [10]. We use the model architecture of a binary Helmholtz Machine with layers of sizes 300, 200, 100, 75, 50, 35, 30, 25, 20, 15, 10, 10, used also by Bornschein et al. [9] to achieve the state of the art performance on the dataset. The training is performed without data augmentation, with binary variables in $\{-1, 1\}$.



(a) miniMNIST B. probs (b) miniMNIST BSt. probs (c) miniMNIST samples

Fig. 2: miniMNIST Dataset examples

The acronyms that we are using are: WS for Wake-Sleep, NWS for the Natural Wake-Sleep, RWS for the Reweighted Wake-Sleep, and NRWS for the Reweighted Wake-Sleep with the natural gradient. All experiments were run with CUDA optimized Tensorflow on Nvidia GTX1080 Ti GPUs. Our implementation is available at <https://github.com/rist-ro/argo>.

miniMNIST

After hyperparameter tuning we compare two different strategies to learn a binary dataset. The first approach is to simply binarize all the samples from the dataset once, by rounding to 0,1, which we call **B**. This technique is used for benchmarking usually and on average have smaller log likelihoods. The second technique, Binary Stochastic or **BSt**, is to take the gray values as the means to a Bernoulli distribution, for each sample from the dataset and for each pixel in the image. At each training step we sample from the distributions, thus we get a range of samples, from a single image, which together approximate the original continuous example better than **B**. In Fig 2 (a) and (b) we see samples from models thought with the differing techniques.

DS	alg.	samples	lr	damping factor	IS log-likelihood	avg time/epoch
Bin	WS	10	0.02	-	-29.337	34s
	RWS	10	0.05	-	-28.695	43s
	NRWS	10	0.002	0.05	-27.606	69s
BSt	WS	10	0.02	-	-38.232	38s
	RWS	10	0.005	-	-37.811	45s
	NRWS	10	0.002	0.05	-36.578	70s

Table 1: Importance Sampling estimation of the log-likelihood with 10000 samples for different algorithms after 500 epochs of training with SGD.

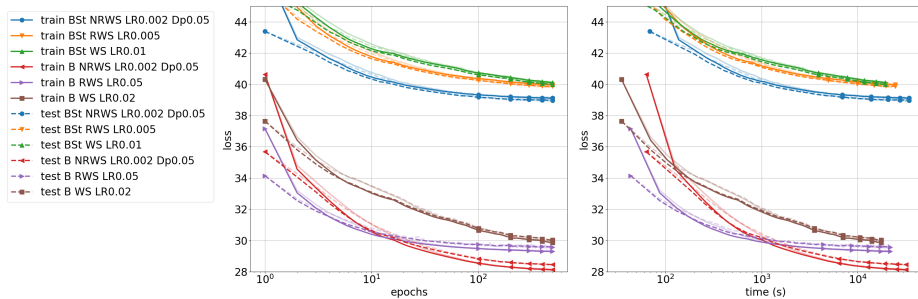


Fig. 3: The loss of training miniMNIST until convergence with **B** and **BSSt**, with the algorithms **WS**, **RWS** and **NRWS** with the layers of the size 100,50,20,10,10. On the left the convergence in epochs and on the right convergence in real life seconds, both in log-scale.

In Fig 3 we compare the loss curves for three different models **WS**, **RWS** and **NRWS** and the two strategies and in Table 1 we report the importance sampled approximation of the log-likelihood. We can see that in all cases the **NRWS** eventually outperforms both models both in achieving the better minimum, as well as in the rate of convergence and wall-clock time. Moreover, a clear advantage is visible early on in the training, in the case of the **B** from the 12th epoch and in **BSSt** from the very beginning.

MNIST

In Fig. 4 and Table 2 we report results of experiments on the MNIST dataset with reasonable parameters for each individual algorithm, based on our hyperparameter tuning. We fix the learning rates to 0.02 and the damping factor to 0.1 for natural gradient methods, all experiments are performed with a **B** binarized dataset, per the benchmarks in the other papers [10, 9].

In Fig. 4 we present loss curves during training, for training and validation. The advantage of the **NRWS** in this case comes in the form of convergence to a better minimum. **NRWS** converges faster than their non-geometric counterparts both in epochs but not in time (left and right panel of Fig. 4). Notice that even by increasing the learning rate for **WS** and **RWS** it is not possible to reach the rate of convergence of the natural gradient versions, due to numerical instabilities.

While **NRWS** outperforms the other methods, its most immediate drawback is that in real-time it takes 5 times as long to reach the same amount of epochs as its non-natural counterpart. While the convergence rate and minimum can be a bit more fine-tuned, the wall-clock time cannot be reduced as easily. Reducing the number of samples for the importance weighting results in faster convergence but it would also impact the performance in a negative way.

The increased convergence speed of the natural algorithms might incidentally increase the risk for premature convergence and overfitting, as can be noticed in

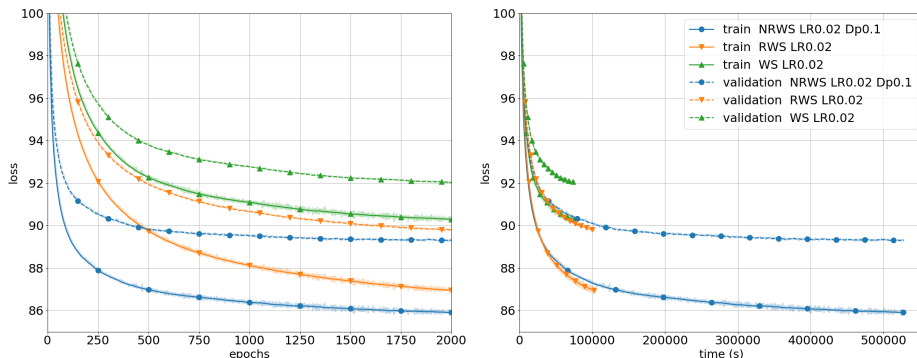


Fig. 4: Training curves for the 3 algorithms with Stochastic Gradient Descent (SGD) plotted till 2000 epochs, continuous lines represent the quantities on the train set, and dashed lines the ones on validation; Left: Loss of algorithms in epochs; Right: Loss of algorithms in wall-clock time (s)

the left panel of Fig. 4, where the gap between train and validation is larger for the NRWS. This phenomenon is known in the literature and has been already reported by other authors in different contexts [27, 17]. The natural gradient, by pointing in the steepest direction with respect to the Fisher-Rao metric, allows for higher rates of convergence, however at the same time it might incur in premature convergence and thus reduce generalization properties.

We begin by comparing our SGDs implementations of WS, RWS and NRWS with state-of-the-art [10, 9], see Table 2. Implementations from the literature also take advantage of accelerated gradient methods, such as ADAM[21], learning-rate decay (from 10^{-3} to 3×10^{-4}) and an increased number of samples towards the end of the training (from 10 to 100), in order to achieve better results. While further hyperparameter tuning could be successfully employed to improve our reported results, as well as variable learning rates, and number of samples [9], this is out of the scope of the present paper.

alg.	samples	lr	damping f.	log-likelihood	avg time/epoch
WS	10	0.02	-	-89.84	37s
RWS	10	0.02	-	-86.168	50s
NRWS	10	0.02	0.1	-86.138	250s
VAE [22]	-	-	-	≈ -89.5	-
RWS [10]	10-100	0.001-0.0003	-	≈ -86.0	-
BiD [9]	10-100	0.001-0.0003	-	≈ -85.0	-

Table 2: Importance Sampling estimation of the log-likelihood with 10000 samples for different algorithms after training till convergence with SGD. The values for VAE, RWS and BiD(Bidirectional Helmholtz Machine) are reported from [9]

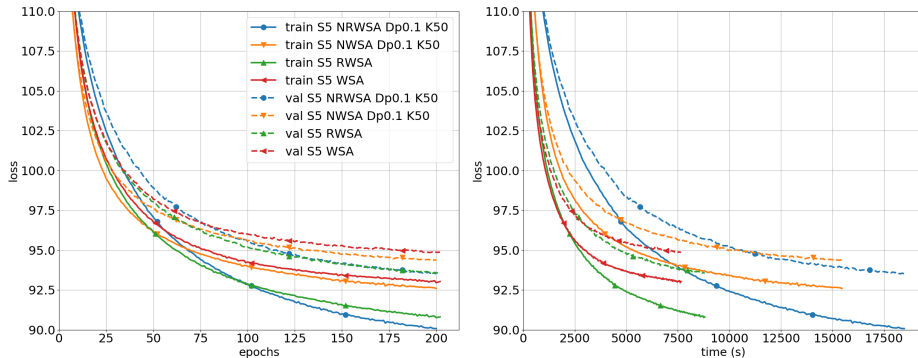


Fig. 5: Training curves for the 4 algorithms with Adaptive Momentum (ADAM), continuous lines represent the quantities on the train set, and dashed lines the ones on validation; Left: Loss of algorithms in epochs; Right: Loss of algorithms in wall-clock time (s);

Additionally, we tested the algorithms using the ADAM optimizer [21]. In Fig. 5 we see that the NWS and NRWS algorithms seem to not take advantage of the adaptive momentum and instead lose in convergence speed. The adaptive steps and the accumulated momentum of ADAM are implicitly assuming an Euclidean metric in the tangent space, which is clearly not the geometrically correct approach. This motivates the exploration of adaptive riemannian gradient methods for the Natural Wake-Sleep algorithms, as a future work.

7 Conclusions

We showed how the graphical structure of Helmholtz Machines allows the efficient computation of the Fisher matrix and thus the natural gradient during training, by exploiting the locality of the connection matrix. In such models it is not required to introduce any extra conditional independence assumption between random variables for computing the natural gradient, since the exact computation can be managed analytically due to the sparse structure.

We introduced the Natural Wake-Sleep (NWS) algorithm along with its reweighted version (NRWS). We demonstrated a convergence improvement during training for standard gradient descent, over their respective state-of-the-art baselines, WS and RWS. The K -step update version of the Natural Wake-Sleep algorithm showed considerable speed-up in terms of training time, while maintaining optimization performances. We noticed how the enhanced convergence speed resulting from the application of the natural gradient might lead to a more pronounced overfitting. The problem of generalization can be tackled in several ways, and studying how to better close the gap between the train and validation loss in NWS and NRWS will be object of further studies. Possible approaches include for example additional tuning of hyperparameters, exploring weight regularization and time dependent damping factor and learning rate.

Moreover, we plan to further study ways to obtain a better estimation of the Fisher matrix. Additional techniques to refine and accumulate the Fisher matrix estimation over time would be beneficial for the training, as well as different ways to obtain samples for the Fisher matrix estimation through importance sampling, thus reweighting the estimation of the Fisher matrix. When using the ADAM optimizer, NWS and NRWS seem to lose the speed advantage over their non-geometric counterparts. This encourages the exploration of adaptive gradient methods for the Natural Wake-Sleep algorithms in which the Fisher-Rao metric is explicitly considered for the momentum accumulation and the adaptive step. Comparing our methods to newer variants of the WS algorithm such as the Memoised WS [18] and the Amortised WS [33] also constitutes future work. As a final remark, we highlight that since the computation of the Fisher matrix is only dependent on the underlying statistical model, as a consequence other algorithms for the training of HMs could benefit from the use of the natural gradient, such as Bidirectional Helmholtz Machine [9].

8 Acknowledgements

This work was supported by the DeepRiemann project, co-funded by the European Regional Development Fund and the Romanian Government through the Competitiveness Operational Program 2014-2020, Action 1.1.4, project ID P-37.714, contract no. 136/27.09.2016.

References

- [1] Shun-ichi Amari. Differential-geometrical methods in statistics. *Lecture Notes on Statistics*, 28:1, 1985.
- [2] Shun-ichi Amari. Neural learning in structured parameter spaces-natural riemannian gradient. In *Advances in neural information processing systems*, pages 127–133, 1997.
- [3] Shun-Ichi Amari. Natural gradient works efficiently in learning. *Neural computation*, 10(2):251–276, 1998.
- [4] Shun-ichi Amari. *Information geometry and its applications*, volume 194. Springer, 2016.
- [5] Shun-ichi Amari and Hiroshi Nagaoka. *Methods of information geometry*, volume 191. American Mathematical Soc., 2000.
- [6] Nihat Ay. Locality of global stochastic interaction in directed acyclic networks. *Neural Computation*, 14(12):2959–2980, 2002.
- [7] Nihat Ay, Jürgen Jost, Hông Vân Lê, and Lorenz Schwachhöfer. *Information geometry*, volume 64. Springer, 2017.
- [8] Yoshua Bengio. Learning deep architectures for ai. *Foundations and Trends in Machine Learning*, 2(1):1–127, 2009.
- [9] Jorg Bornschein, Samira Shabanian, Asja Fischer, and Yoshua Bengio. Bidirectional Helmholtz Machines. *arXiv:1506.03877 [cs, stat]*, June 2015. arXiv: 1506.03877.
- [10] Jrg Bornschein and Yoshua Bengio. Reweighted Wake-Sleep. *arXiv:1406.2751 [cs]*, June 2014. arXiv: 1406.2751.

- [11] Peter Dayan, Geoffrey E Hinton, Radford M Neal, and Richard S Zemel. The helmholtz machine. *Neural computation*, 7(5):889–904, 1995.
- [12] Guillaume Desjardins, Razvan Pascanu, Aaron Courville, and Yoshua Bengio. Metric-free natural gradient for joint-training of boltzmann machines. *arXiv preprint arXiv:1301.3545*, 2013.
- [13] Guillaume Desjardins, Karen Simonyan, Razvan Pascanu, et al. Natural neural networks. In *Advances in Neural Information Processing Systems*, pages 2071–2079, 2015.
- [14] Xavier Glorot and Yoshua Bengio. Understanding the difficulty of training deep feedforward neural networks. In *Proceedings of the thirteenth international conference on artificial intelligence and statistics*, pages 249–256, 2010.
- [15] Ian Goodfellow, Yoshua Bengio, and Aaron Courville. *Deep learning*. MIT press, 2016.
- [16] Alex Graves. Practical variational inference for neural networks. In *Advances in neural information processing systems*, pages 2348–2356, 2011.
- [17] Roger Grosse and James Martens. A kronecker-factored approximate fisher matrix for convolution layers. In *International Conference on Machine Learning*, pages 573–582, 2016.
- [18] Luke B Hewitt, Tuan Anh Le, and Joshua B Tenenbaum. Learning to learn generative programs with memoised wake-sleep. *arXiv preprint arXiv:2007.03132*, 2020.
- [19] Geoffrey E Hinton, Peter Dayan, Brendan J Frey, and Radford M Neal. The "wake-sleep" algorithm for unsupervised neural networks. *Science*, 268(5214):1158–1161, 1995.
- [20] Geoffrey E Hinton, Simon Osindero, and Yee-Whye Teh. A fast learning algorithm for deep belief nets. *Neural computation*, 18(7):1527–1554, 2006.
- [21] Diederik P Kingma and Jimmy Ba. Adam: A method for stochastic optimization. *arXiv preprint arXiv:1412.6980*, 2014.
- [22] Diederik P Kingma and Max Welling. Auto-encoding variational bayes. *ICLR, arXiv:1312.6114*, 2014.
- [23] Kevin G Kirby. A tutorial on helmholtz machines. *Department of Computer Science, Northern Kentucky University*, 2006.
- [24] Tuan Anh Le, A Kosiorek, N Siddharth, Yee Whye Teh, and Frank Wood. Revisiting reweighted wake-sleep for models with stochastic control flow. 2019.
- [25] Yann LeCun, Corinna Cortes, and CJ Burges. Mnist handwritten digit database. 2010.
- [26] Wu Lin, Mohammad Emtiyaz Khan, Nicolas Hubacher, and Didrik Nielsen. Natural-gradient stochastic variational inference for non-conjugate structured variational autoencoder. 2017.
- [27] James Martens and Roger Grosse. Optimizing neural networks with kronecker-factored approximate curvature. In *International conference on machine learning*, pages 2408–2417, 2015.
- [28] Radford M Neal. Connectionist learning of belief networks. *Artificial intelligence*, 56(1):71–113, 1992.
- [29] Yann Ollivier. Riemannian metrics for neural networks i: feedforward networks. *Information and Inference: A Journal of the IMA*, 4(2):108–153, 2015.
- [30] H Park, S.-I Amari, and K Fukumizu. Adaptive natural gradient learning algorithms for various stochastic models. *Neural Networks*, 13(7):755 – 764, 2000.
- [31] Danilo Jimenez Rezende, Shakir Mohamed, and Daan Wierstra. Stochastic back-propagation and approximate inference in deep generative models. *arXiv preprint arXiv:1401.4082*, 2014.

- [32] Ke Sun and Frank Nielsen. Relative fisher information and natural gradient for learning large modular models. In *Proceedings of the 34th International Conference on Machine Learning-Volume 70*, pages 3289–3298. JMLR. org, 2017.
- [33] Li K Wenliang, Theodore Moskovitz, Heishiro Kanagawa, and Maneesh Sahani. Amortised learning by wake-sleep. *arXiv preprint arXiv:2002.09737*, 2020.
- [34] Guodong Zhang, Shengyang Sun, David Duvenaud, and Roger Grosse. Noisy natural gradient as variational inference. *arXiv preprint arXiv:1712.02390*, 2017.

A Fisher Matrix of a Sigmoid Belief Network

In a Sigmoid Belief Network with L layers, the joint probability of all the neurons in the network can be written as

$$p(h) = p(h^{(0)}) \prod_{i=1}^L p(h^{(i)} | h^{(i-1)}), \quad (18)$$

where $h^{(i)} \in \mathbb{R}^{l_i}$ is the boolean vector representing the layer i with size l_i , and h is the collection of all the layers in the network. For each neuron r of the layer i , $p(h_r^{(i)} | h^{(i-1)})$ is a Bernoulli, depending on the previous layer

$$p(h_r^{(i)} | h^{(i-1)}) = \sigma(W_r^{(i)} \cdot h^{(i-1)} + b_r^{(i)})^{h_r^{(i)}} \left(1 - \sigma(W_r^{(i)} \cdot h^{(i-1)} + b_r^{(i)})\right)^{1-h_r^{(i)}} \quad (19)$$

where $W_r^{(i)} \in \mathbb{R}^{l_{i-1}}$ is a vector of weights for the neuron r of the layer i , and $b_r^{(i)}$ is a bias. Equation 19 can be also written in compact form as

$$p(h_r^{(i)} | h^{(i-1)}) = \sigma(\tilde{W}_r^{(i)} \cdot \tilde{h}^{(i-1)})^{h_r^{(i)}} \left(1 - \sigma(\tilde{W}_r^{(i)} \cdot \tilde{h}^{(i-1)})\right)^{1-h_r^{(i)}}, \quad (20)$$

where $h^{(i-1)}$ and $W_r^{(i)}$ have been augmented with 1 and $b_r^{(i)}$, respectively. The second derivative of the ln of (20) is

$$\frac{\partial^2}{\partial \tilde{W}_{r_l}^{(i)} \partial \tilde{W}_{r_m}^{(i)}} \ln p(h_r^{(i)} | h^{(i-1)}) = -\sigma(\tilde{W}_r^{(i)} \cdot \tilde{h}^{(i-1)}) \left(1 - \sigma(\tilde{W}_r^{(i)} \cdot \tilde{h}^{(i-1)})\right) \tilde{h}_l^{(i-1)} \tilde{h}_m^{(i-1)}. \quad (21)$$

This leads to a natural block structure, the Fisher matrix with respect to the weights $\tilde{W}_r^{(i)}$ is

$$\begin{aligned} F[\tilde{W}_r^{(i)}] &= \mathbb{E}_{p(h)} \left[-\frac{\partial^2}{\partial \tilde{W}_r^{(i)} \partial \tilde{W}_r^{(i)}} \ln p(h_r^{(i)} | h^{(i-1)}) \right] \\ &= \mathbb{E}_{p(h)} \left[\sigma(\tilde{W}_r^{(i)} \cdot \tilde{h}^{(i-1)}) \left(1 - \sigma(\tilde{W}_r^{(i)} \cdot \tilde{h}^{(i-1)})\right) \tilde{h}^{(i-1)} \tilde{h}^{(i-1)\top} \right]. \end{aligned} \quad (22)$$

In case we would use +1 and -1 instead

$$p(h_r^{(i)} | h^{(i-1)}) = \sigma(h_r^{(i)} \tilde{W}_r^{(i)} \cdot \tilde{h}^{(i-1)}), \quad (23)$$

and in the end the Fisher Matrix would be the same. Try to believe.

B Hyperparameter tuning for 3by3, miniMNIST and MNIST

In addition to miniMNIST and MNIST use the ThreeByThree (denoted in the following as 3by3) synthetic dataset introduced by Kirby [23] which consists of

a 3by3 grid with vertical and horizontal patterns, represented in Fig. 9a (left). The advantage of this dataset is that the true KL divergence value between the *generation distribution* p and the *true distribution* of the data p^* can be calculated very precisely, and we don't have to rely solely on the approximation of the log-likelihood which is traditionally used to evaluate generative models.

Learning Rate and Damping Factor

Ideally we want to find the smallest damping factor which still maintains the optimization stable. Too large damping factors lead to an optimization similar to the non natural algorithms, while too small damping factors lead to a large conditioning number in the estimated Fisher matrix, whose inversion then carries serious numerical issues. This behaviour can be seen clearly in Fig. 6. We searched empirically for the right combination of learning rate and damping factor leading to the best convergence rate.

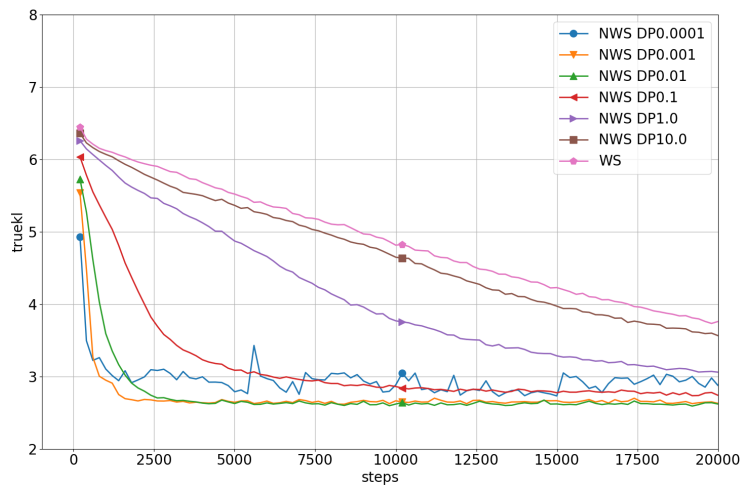


Fig. 6: The loss with different damping values for the 3by3 dataset.

For the 3by3 dataset we determined a range of 0.001 – 0.1 for damping values that outperform the vanilla algorithm (Fig. 6). As one can observe, with very low damping the algorithm converges almost instantly but the loss remains noisy, as each small modification in the Fisher matrix is amplified when applied to the gradient. Large values however lead to convergence that is similar to the one of WS. From this general range the parameter has to be fine-tuned for each dataset/model, to determine the appropriate combination of learning rate versus damping factor.

In Fig. 7 and Fig. 8 we compare different learning rates and damping factors on a smaller architecture to determine the appropriate quantities for optimal

convergence in the case of the miniMNIST and MNIST. We determine that the appropriate damping factor for this dataset with similar models is around $0.005 - 0.1$, with a learning rate in the neighbourhood of $0.005 - 0.02$.

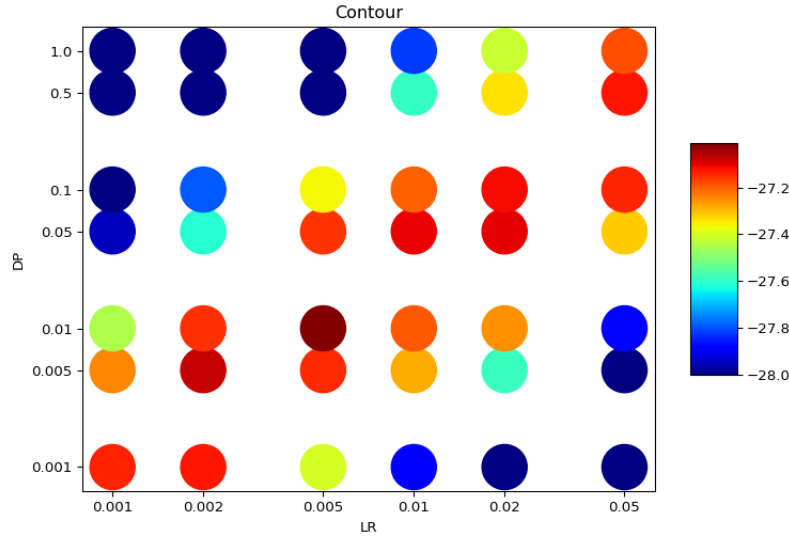


Fig. 7: The minimum loss of experiments in relation to Learning rate and Damping factor, on a model with 100, 50, 20, 10, 10 layers.

We can notice the expected linear relation between learning rate and damping factor. When we grow the damping factor, we can also grow the learning rate up to a given point. The explanation for this phenomenon is that (as shown in section 5.1) the smaller the damping, the closer the algorithm is to following the geometry of the manifold defined by the statistical model, thus smaller steps lead to better improvements.

We also observe a correlation between the size of the image and the magnitude of the damping factor, which is to be expected. The larger the image in the first layer, that much more samples are needed to approximate its Fisher matrix accurately. In the case when the number of samples cannot be grown anymore (remember the complexity of the algorithm grows quadratically with the number of samples), the larger damping factor is needed so the matrix can have a reasonable conditioning number.

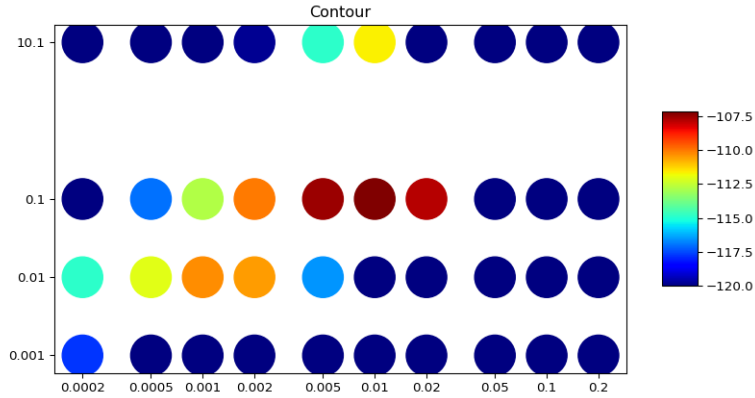


Fig. 8: The minimum loss of experiments in relation to Learning rate and Damping factor, on a model with 200,100,10 layers.

K-step

Once obtained the best combination of hyperparameters for the Natural Wake-Sleep Optimizer, we explore the possibility to compute the Fisher only every K -steps and thus speed up the computational time of the algorithm. In Fig. 9b we see the changes in the loss on the validation set for MNIST for a fixed learning rate and damping factor. We observe that for a K -steps the algorithm speeds up significantly, but loses stability at very high values, which is most noticeable in the case of $K = 1000$ steps, and to a lesser degree for $K = 500$. Consequently we can use a K -step in the range of $[1, 100]$ without noticeable impact on the performance of the algorithm. In our experiments we used $K = 50$ or $K = 100$.

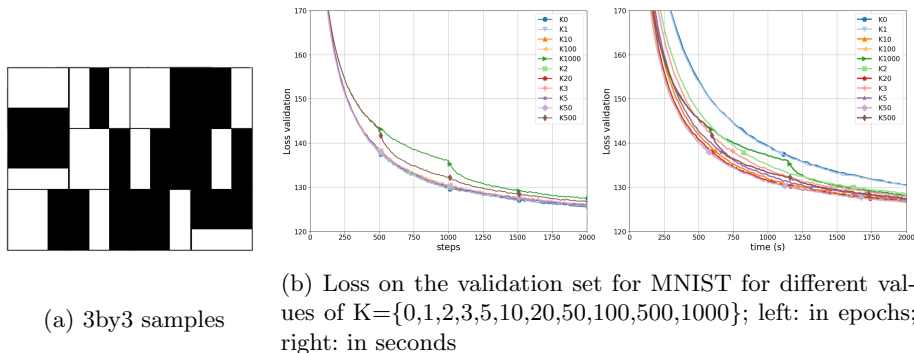


Fig. 9: Left: 3x3 example; Right: Loss in function of K-step